AIP | Journal of Applied Physics

Field emission from single-, double-, and multi-walled carbon nanotubes chemically attached to silicon

Cameron J. Shearer, Adam Fahy, Matthew G. Barr, Katherine E. Moore, Paul C. Dastoor et al.

Citation: J. Appl. Phys. **111**, 044326 (2012); doi: 10.1063/1.3687363
View online: http://dx.doi.org/10.1063/1.3687363
View Table of Contents: http://jap.aip.org/resource/1/JAPIAU/v111/i4
Published by the American Institute of Physics.

Field emission from single-, double-, and multi-walled carbon nanotubes chemically attached to silicon

Cameron J. Shearer,[1,a)] Adam Fahy,[2] Matthew G. Barr,[2] Katherine E. Moore,[1] Paul C. Dastoor,[2] and Joseph G. Shapter[1,b)]
[1]*Centre for Nanoscale Science and Technology, School of Chemical and Physical Sciences, Flinders Centre for NanoScale Science and Technology, Adelaide 5042, South Australia*
[2]*Centre for Organic Electronics, School of Physics, University of Newcastle, Callaghan, New South Wales 2308, Australia*

(Received 30 September 2011; accepted 2 January 2012; published online 28 February 2012)

The chemical attachment and field emission (FE) properties of single-walled carbon nanotubes (SWCNTs), double-walled carbon nanotubes (DWCNTs), and multi-walled carbon nanotubes (MWCNTs) chemically attached to a silicon substrate have been investigated. A high density of CNTs was revealed by atomic force microscopy imaging with orientation varying with CNT type. Raman spectroscopy was used to confirm the CNT type and diameter on the surfaces. The field emission properties of the surfaces were studied and both current-voltage and Fowler-Nordheim plots were obtained. The SWCNTs exhibited superior FE characteristics with a turn-on voltage (E_{to}) of 1.28 V μm^{-1} and electric field enhancement factor (β) of 5587. The DWCNT surface showed an E_{to} of 1.91 V μm^{-1} and a β of 4748, whereas the MWCNT surface exhibited an E_{to} of 2.79 V μm^{-1} and a β of 3069. The emission stability of each CNT type was investigated and it was found that SWCNTs produced the most stable emission. The differences between the FE characteristics and stability are explained in terms of the CNT diameter, vertical alignment, and crystallinity. The findings suggest that strength of substrate adhesion and CNT crystallinity play a major role in FE stability. Comparisons to other FE studies are made and the potential for device application is discussed. © *2012 American Institute of Physics*. [doi:10.1063/1.3687363]

I. INTRODUCTION

Electron field emission (FE) from carbon nanotubes (CNTs) has been an intensely researched topic since the initial reports of the phenomenon in 1995.[1] This high level of interest is predominantly due to the inherent properties of CNTs such as the high conductivity and large aspect ratio, which lead to a high maximum current output and low turn-on voltage (E_{to}).[2,3] In order to utilize the full effects of the large aspect ratio of the CNT, it is advantageous to have the CNT vertically aligned upon a substrate. Vertical alignment increases the electric field enhancement (β) around the CNT, which reduces the macroscopic applied field required for field emission.[4]

CNTs can be distinguished as a single-walled carbon nanotube (SWCNT), a double-walled carbon nanotube (DWCNT), or a multi-walled carbon nanotube (MWCNT), depending upon the number of concentric graphene cylinders present. Field emission from the different CNT types is thought to vary significantly between the CNT types as a result of the difference in diameter, and hence aspect ratio. However, very few direct experimental comparisons exist between the field emission from the various CNT types. The accepted theory is that SWCNTs exhibit the best FE characteristics, whereas MWCNTs produce the most stable emission.[3] This hypothesis is a consequence of the single shelled SWCNT exhibiting the highest aspect ratio, whereas the multiple shelled MWCNT is more robust and less affected by common FE degradation mechanisms such as ion bombardment.[5,6] Recent reports have shown that DWCNTs have the potential to have greater FE characteristics than SWCNTs, whereas their extra wall should also improve their emission stability.[7] For this reason, direct experimental comparison of the FE properties of the three CNT types is required.

Surface bound CNTs for FE studies are commonly prepared via chemical vapor deposition (CVD) growth of CNTs[8] or by incorporating CNTs into a paste and printing them onto a surface.[6,9] CVD growth of CNTs leads to a greater control of alignment with the ability to produce an array of vertically aligned CNTs. However, it is difficult to grow the different CNT types without vastly changing the experimental procedure.[10] In addition, the substrate to CNT adhesion is limited to relatively weak noncovalent interactions between CNT, catalyst nanoparticle and substrate.[5,11] The screen printing method is easily interchangeable between the CNT types but there is little control over the alignment of the CNTs.

Recent work has demonstrated the chemical attachment of SWCNTs to silicon in order to improve adhesion between CNT and substrate.[10,12] These surfaces have shown promise in the fields of electrochemistry,[13] photovoltaics,[14] and we have recently reported on field emission.[15] In our initial report we showed the chemical attachment of SWCNTs to silicon is an upscaleable approach to producing a field emission device with low E_{to} (~1.5 V μm^{-1}), high β (~6000) and good emission stability.[15]

Here, we chemically attach SWCNTs, DWCNTs, and MWCNTs to silicon in order to determine and directly

a)Electronic mail: Cameron.Shearer@flinders.edu.au.
b)Electronic mail: Joe.Shapter@flinders.edu.au.

compare their field emission properties. The Si-DWCNT surfaces have the potential to improve upon the field emission properties obtained for the Si-SWCNT surface. The chemical attachment of the cheaper MWCNT (when compared to DWCNT and SWCNT) could potentially produce a more cost effective field emission substrate without significantly decreasing the field emission properties.

II. MATERIALS AND METHODS

A. Carbon nanotube functionalization

The CNT chemical attachment scheme (Fig. 1) details how ester coupling is achieved between carboxylic acid functionalized CNTs and a hydroxyl terminated silicon wafer. To complete this attachment the otherwise inert CNTs must be functionalized and the inert silicon oxide covered Si wafer must be hydroxylated. Each specific carbon nanotube type was functionalized following a slightly different method that was tailored specifically to create a stable CNT suspension. Immersion in acidic solutions was completed at CNT concentrations of 1 mg ml^{-1}.

SWCNTs (P2, >90% carbonaceous purity, 1.4 nm diameter, Carbon Solutions Inc.) were functionalized/cut by incubation in a solution of 3:1 (v/v) H_2SO_4 (98%, Aldrich):HNO_3 (70%, Aldrich) in an Elma S30 H ultrasonic bath kept at 0 °C for 8 h. The sonication of CNTs in strong acid solutions is known to both functionalize with carboxylic acid groups and decrease their lengths.[16]

DWCNTs (>90% carbonaceous purity, >60% DWCNT purity, >5 nm outer diameter, ShenZhen Nanotech Port Co., China) were functionalized/cut by a two-step process. The first was reflux in 3 M solution of HNO_3 for 16 h. The DWCNTs were then filtered through a 0.45 μm polytetrafluoroethylene (PTFE) membrane (Adelab Scientific, Australia) followed by sonication at 0 °C for 2 h in a solution of 3:1 (v/v) H_2SO_4:HNO_3.

MWCNTs (L-MWNT-2040, >95% carbonaceous purity, 20–40 nm outer diameter, Shenzhen Nanotech Port Co. Ltd., China) were functionalized following a three-step process. First they were refluxed in 3 M HNO_3 for 3 h. They were then filtered through a 0.45 μm PTFE filter followed by sonication in 7:3 H_2SO_4:HNO_3 mixed acid for 3 h at room temperature. Finally the MWCNTs were filtered again and sonicated in a solution of 2 M HCl (36%, Ajax Finechem, Australia) for 20 min.

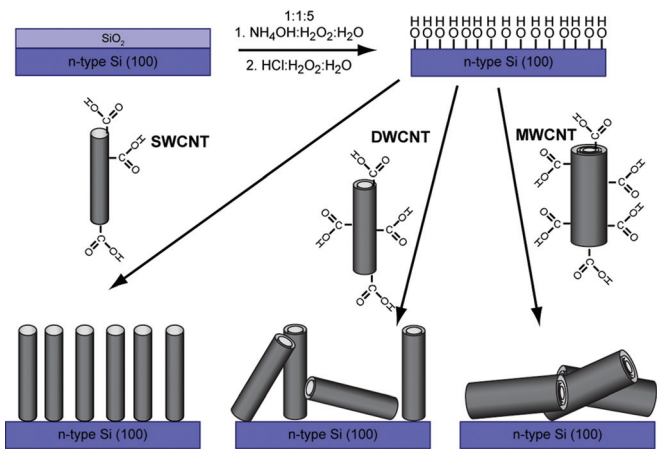

FIG. 1. (Color online) Schematic of the attachment method of SWCNTs, DWCNTs, and MWCNTs to silicon.

Following the final functionalization steps the CNTs were filtered a final time through a PTFE membrane and washed with water (milliQ, 18 MΩ cm) until a neutral filtrate *p*H was obtained. The CNTs were then dried in an oven at 100 °C overnight to remove residual water. The dried functionalized CNTs were then dispersed in dimethyl sulfoxide (DMSO, 99.9%, ACS Spectroscopic Grade, Sigma–Aldrich) along with dicyclohexylcarbodiimide (DCC, 99% FlukaProduction GmbH) at a concentration of 0.2 mg ml^{-1}. The solutions containing 0.2 mg ml^{-1} of both functionalized CNT and DCC were used for CNT surface attachment to hydroxylated silicon.

B. CNT attachment to silicon

The silicon wafers were hydroxylated following a method similar to the RCA cleaning procedure.[17] Antimony doped *n*-type silicon wafers (0.5 mm thickness, 0.008–0.02 Ω cm, VA Semiconductor) were cut to $\sim 1 \times 1$ or $\sim 0.5 \times 0.5$ cm^2 and were initially ultrasonically cleaned in acetone (99%, Sigma) for 2 min. The Si wafers were then washed with water (MilliQ), dried in a stream of nitrogen and immersed in a solution of 1:1:5 NH_4OH (30%, Sigma-Aldrich):H_2O_2 (30%, Sigma-Aldrich):MilliQ for 20 min at 80 °C. This was followed by washing with MilliQ water, drying in nitrogen and immersing in a 1:1:5 solution of HCl: H_2O_2:MilliQ for 20 min at 80 °C. Each hydroxylated wafer was then washed with MilliQ and dried with nitrogen before being placed in a round-bottomed flask.

Inside a nitrogen filled glovebox, ~2 ml of 0.2 mg ml^{-1} shortened CNT solution in DMSO, containing 0.2 mg ml^{-1} DCC was added to each round-bottomed flask containing a hydroxylated silicon wafer. The flasks were stoppered and wrapped in Parafilm and fiberglass tape to ensure a good seal before being placed in an oven at 80 °C for 2 h (SWCNT) or 24 h (DWCNT/MWCNT). At the appropriate time, the surfaces were removed from the oven and rinsed thoroughly in acetone to remove any unbound reagents and stored in acetone or argon prior to use.

C. Surface characterization

AFM tapping mode images were taken in ambient conditions with a multimode head and a Nanoscope IV controller (Bruker, Santa Barbara, CA). Silicon cantilevers (MikroMasch) with a fundamental resonance frequency of between 300 and 400 kHz were used. Images were obtained using a scan rate of 1 Hz with the parameters of set point, amplitude and feedback control optimized manually for each sample. The images presented have been flattened using Nanoscope IV software. The CNT coverage was calculated using the bearing analysis tool on the Nanoscope IV software with the threshold set manually.

Raman spectra were recorded on a Witec Alpha 300RS confocal Raman microscope fitted with a 532 nm laser (60 mW) using a 100× (0.9 numerical aperture, working

distance 0.23 mm) objective. The spectra were taken as an average of three scans over a collection time of 30 s. The experiments were carried out using Witec Control 1.42 software and the analysis was completed using Witec project 1.90 software.

D. Field emission

Field emission measurements were performed using both 1 and 0.25 cm^2 Si-CNT samples as cathodes. The emitted electrons were collected on a highly polished stainless steel counter electrode under an average ultrahigh vacuum of $\sim 6 \times 10^{-9}$ Torr (range from 1×10^{-9}–1×10^{-8} Torr). The distance between the electrodes was measured to be 1.82 mm using a micrometer screw. A Spellman SL10 high voltage source unit was used to supply the voltage (up to 8000 V). The current produced at the anode was measured using a Keithley 6485 picoammeter. An in-house program written in LabView 8.2 was used to control the voltage and current, as well as record the data. Conditioning of the samples was completed prior to FE sweeps. The conditioning of the samples was completed by manually raising the voltage such that the output current was $\sim$180 μA and then left for 2–5 min until the emission was constant. This procedure stresses the sample and removes adsorbed molecules, making the emission more stable. Current–voltage (I–V) sweeps were obtained by sweeping the voltage from 0 V to a maximum of 8 kV in steps of 50 V with each voltage held for 1 s. Once the current output reached the limiting current of 180 μA the voltage was returned to zero. The stability tests were completed by setting the LabView program to keep the input current constant, simultaneously allowing the LabView program to vary the applied voltage accordingly. The voltage and current produced were measured every second for the duration of the stability test.

III. RESULTS AND DISCUSSION

A. Surface characterization

The chemical attachment and vertical alignment of SWCNTs to silicon and other surfaces has been accomplished previously on numerous occasions and the methodology is well practiced.[10,18] However the chemical functionalization and attachment of DWCNTs and MWCNTs to silicon via the ester attachment described here has not been previously reported. As such, the attachment and alignment of DWCNTs and MWCNTs will be covered in detail.

Chemical attachment and alignment of the CNTs was investigated by AFM. Figure 2(a) shows an AFM image of SWCNTs chemically attached to the silicon surface. Circular features are observed, which are recognized as bundles of vertically aligned SWCNTs. The vertical alignment of SWCNTs following the chemical attachment method has been well documented[19–23] and is attributed to a range of factors including the higher concentration of carboxylic acid groups on the ends of the SWCNTs and the hydrophobic sidewalls of the SWCNTs being repelled by the hydrophilic hydroxylated surface. The vertical alignment is more obvious in the 3D AFM image [Fig. 2(d)]. The SWCNT bundles on

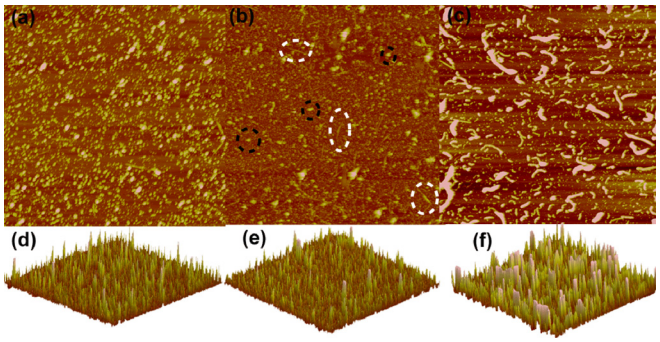

FIG. 2. (Color online) (a–c) Top down and (d–f) 3D AFM images of (a,d) SWCNTs, (b,e) DWCNTs, and (c,f) MWCNTs chemically attached to silicon. Black circles in (b) indicate examples of vertically aligned CNTs, whereas white circles indicate lying down CNTs. All images are 5×5 μm^2 with a z scale of 50 nm.

the surface have an average diameter of 75 $\pm$ 10 nm and cover 35% of the surface.[15]

Figures 2(b) and 2(e) show AFM images of DWCNTs chemically attached to silicon. Both circular and rod-like features are observed on the surface corresponding to both vertically aligned and lying down (horizontally aligned) bundles of DWCNTs. Some examples of vertically aligned (black circles) and lying down (white circles) have been highlighted in Fig. 2(b) to highlight the two different types of features. The presence of both lying down and vertically aligned DWCNTs is considered to be due to the DWCNT functionalization process. During functionalization, carboxylic acid groups will initially attack either the stress sites at the ends of the nanotubes or defect sites on the sidewalls of the CNT. The production process used for the purchased DWCNTs (CVD) is known to create more defect sites along the sidewalls than that used for SWCNT production (arc discharge). The defect sites on the sidewalls of the DWCNT that are present after fabrication will be oxidized during the functionalization process leading to a DWCNT that is decorated with carboxylic acid functional groups both at its ends and along its sidewalls.[24,25] When these DWCNTs are bonded to the silicon surface, attachment can occur at either their ends or their sidewalls, leading to both vertical and horizontal alignment. The coverage on the surface was $\sim$40% and the diameter of the bundles of DWCNTs was calculated to be 68 $\pm$ 20 nm.

The attachment of MWCNTs leads almost exclusively to a lying down geometry [Figs. 2(c) and 2(f)], which is attributed to the MWCNTs having a higher initial sidewall defect site population than the DWCNTs and therefore having a higher concentration of sidewall functionalization after the chemical oxidation process, which results in the side-on attachment of the MWCNTs. The MWCNTs were found to cover $\sim$30% of the surface. The average bundle diameter of the MWCNTs was calculated to be 74 $\pm$ 10 nm, which indicates that they exist in bundles of a few MWCNTs.

It was previously found that the CNT coverage had a large effect on the field emission properties of Si-SWCNT surfaces.[15] For this reason the CNT attachment times were carefully chosen to produce a consistent coverage at 35 $\pm$ 5% across the samples investigated. The diameter values obtained

via AFM imaging are an average bundle diameter, not the individual diameter of the CNTs. Each bundle contains CNTs of various lengths and consequently some CNTs are expected to protrude from the surface further than others. The field emission from the surface will be affected by coverage, alignment, and CNT type. The alignment of the CNTs varies between CNT types from vertically aligned for the SWCNTs to horizontal for the MWCNTs. This will affect the electric field enhancement of each. Attempts to increase vertical alignment of both DWCNT and MWCNT surfaces were attempted, such as altering the chemical oxidation process, but were not successful.

Raman spectroscopy was used to confirm the structure/type of the CNTs chemically attached to the silicon surface. Figure 3(a) shows a Raman spectrum of the Si-SWCNT surface; the CNT peaks observed in the spectrum are attributed to the radial breathing mode (RBM, 175 cm^{-1}), the disorder-induced mode (D-band, 1337 cm^{-1}), the graphitic mode (G-band), which is split into the G^--band (1570 cm^{-1}) and the G^+-band (1586 cm^{-1}), and the overtone of the D-band (G′-band 2664 cm^{-1}).[26] The region from 200 to 1200 cm^{-1} is dominated by peaks from the silicon surface and no SWCNT Raman peaks are discernable. The Raman data confirms the presence of SWCNTs on the surface due to the single RBM peak, which indicates that only a single diameter of SWCNT is present. The inset shows the RBM peak in detail. The position of the RBM (ω_{RBM}) gives information on the diameter of the SWCNTs using the expression:

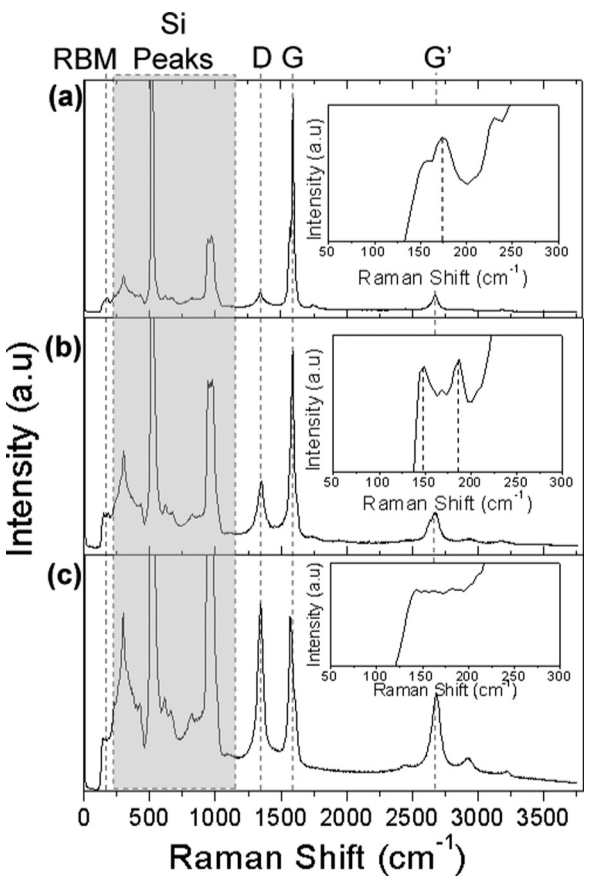

FIG. 3. Raman spectra of (a) SWCNTs, (b) DWCNTs, and (c) MWCNTs chemically attached to silicon with zoom of RBM peak region (insets).

$\omega_{RBM} = A/d_t + B$, where d_t is the diameter of the SWCNTs investigated and A, B are parameters dependent upon the CNT environment.[26] For bundled SWCNTs on a Si surface at a high density A and B have previously been calculated to be 223.5 cm^{-1} nm and 25.5 cm^{-1} respectively.[27] Using these values the diameter of SWCNTs on the Si surface was calculated to be 1.5 nm, (Table 1) which is in agreement with the diameter quoted by the supplier (1.4 nm). A common calculation in Raman spectroscopy of CNTs is the D/G ratio. The D-band is due to scattering from sp^3 bonded carbon (such as in defect sites in the CNT sidewall) and is an indicator of disorder or functionalization within the CNT and thus its relative height when compared to the graphite like G-band is used as a measure of CNT crystallinity. Lower values for D/G indicate higher CNT crystallinity. The Si-SWCNT electrode recorded a D/G value of 0.08, (Table 1) which is in the lower range of values obtained in prior Raman studies indicating that there is little sidewall functionalization of the SWCNTs.[26]

A Raman spectrum of the Si-DWCNT surface is shown in Fig. 3(b). Although the peaks observed are predominately the same as for the SWCNT surface, two key differences are observed. First, the RBM now consists of two peaks at 150 cm^{-1} (1.8 nm) and 187 cm^{-1} (1.38 nm) indicating that there is more than one diameter of CNT present in the sample.[28] More DWCNT Raman peaks are expected to lie in the 250–350 cm^{-1} region of the spectrum. These peaks are not observed in Fig. 3(b) due to the interference of the silicon substrate, but can be observed when the DWCNTs are dropped onto a mica substrate (see the supplemental material[29]). Similarly, CNTs of diameters greater than 2 nm are expected at a Raman shift values lower than 150 cm^{-1}, but are not observed because the filter within the Raman spectrometer removes all signal below 150 cm^{-1}. The many Raman peaks observed corresponding to low diameter CNTs supports the manufacturer's claim that DWCNTs with an outer diameter of <5 nm are present on the Si-DWCNT electrode. The second difference in Raman spectra between the Si-SWCNT and Si-DWCNT electrodes is the increase in the D/G ratio to 0.27, which arises from an increased functionalization of the DWCNT outer walls and a decrease in CNT crystallinity, and supports our explanation for the presence of both vertically and horizontally aligned DWCNTs on the surface.

The Raman spectrum of the Si-MWCNT electrode is displayed in Fig. 3(c). The spectrum is vastly different to that of the SWCNTs and DWCNTs, the difference is mainly due to the change in diameter of the CNTs where larger diameter MWCNTs do not exhibit RBM peaks.[26] A second difference is the size of the D-band, which has become much larger with a D/G ratio of 1.04 compared to 0.08 for SWCNT and 0.27 for the DWCNT surface. The apparent large number of defect sites, as shown by the large D-band, is a common observation in MWCNTs, where the imperfect fabrication process leads to a reduction in crystallinity within the CNT lattice.[30] The high D/G ratio also suggests that there is a large amount of sidewall functionalization on the MWCNTs, which contributes to the exclusive lying down geometry of the surface observed by AFM imaging.

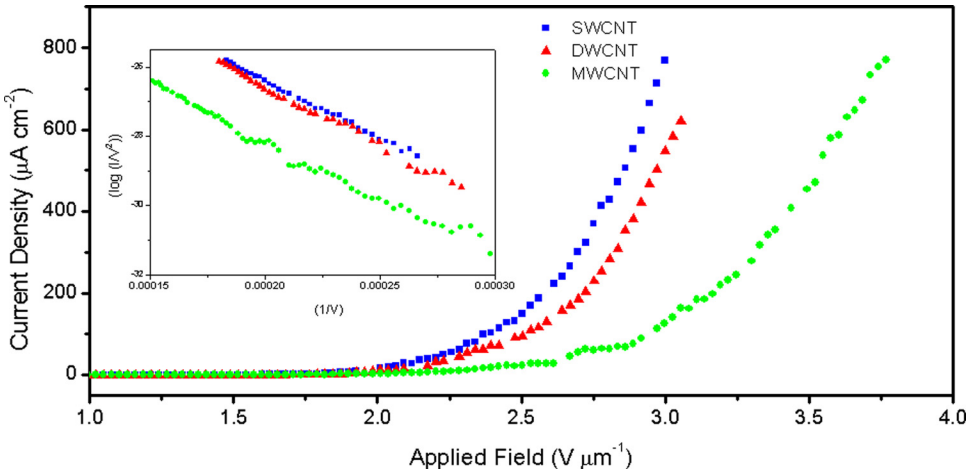

FIG. 4. (Color online) Field emission sweeps for SWCNTs, DWCNTs, and MWCNTs (as indicated by legend) chemically attached to silicon with Fowler-Nordheim plots for each CNT type (inset).

B. Field emission properties

Field emission sweeps for Si-SWCNT, Si-DWCNT, and Si-MWCNT electrodes along with their F–N plots are shown in Fig. 4. All samples exhibited field emission with linear F–N plots.[31] Small fluctuations are observed, particularly for the Si-MWCNT electrode, and are a consequence of the inhomogeneous nature of the field emitting surface. These small variations most likely arise from a combination of phenomena, such as the variation of CNT tip height/radius as a result of field desorption or evaporation leading to variations in β.[32] The FE sweeps in Fig. 4 all exhibit an exponential shape up to the maximum current recordable on our system (750 μA cm^{-2}). The shape of the FE sweeps suggest that a greater output current could be obtained within a system capable of recording higher current values.

The CNT type had a noticeable effect on both the electric field enhancement and the turn-on voltage as summarized in Table I. The turn-on voltage is the macroscopic field required to obtain a certain output current density. The most commonly used target current density is 10 μA cm^{-2}, which will be used for further discussion. The E_{to} values for 100 and 500 μA cm^{-2} are also shown in Table I for comparison. The electric field enhancement factor is a value for the electric field enhancement around the emitting CNT tip. Values of β were calculated from the slope of the F–N plots following previously described methods ($\mu = 1.9$ eV, $\Phi = 4.8$ eV).[33,34]

There is a clear correlation between FE properties with CNT diameter. The lowest diameter SWCNTs exhibit the highest β and lowest E_{to}, whereas the largest diameter MWCNTs showed the lowest β and highest E_{to}. The effect of diameter is coupled with the level of vertical alignment of the CNTs, as shown by AFM imaging (Fig. 2), the Si-SWCNT exhibits the greatest degree of vertical alignment, whereas the Si-MWCNT shows no vertical alignment. This observed correlation is consistent with current theory where the CNTs with the highest aspect ratio exhibit the best field emission properties.[35]

Comparison of the field emission of the SWCNT chemically attached to silicon surfaces has been completed in detail previously.[15] Briefly, the average FE characteristics of SWCNT emitters rarely have E_{to} values below 1.5 V μm^{-1} and β values are seldom higher than 5000. By comparison, our Si-SWCNT surfaces display an E_{to} of 1.29 V μm^{-1} and a β of 5587 indicating that the surface is an elite field emitting device.[6,36] E_{to} and β for DWCNTs are often similar to that of SWCNTs due to the small difference in diameter between the two. The field emission of the DWCNT surface presented here compares favorably with other work where values for E_{to} of 1–3 V μm^{-1} and 1000–5000 for β are common.[37–39] MWCNTs are by far the most extensively studied of the CNT types due to their ease of fabrication. However, the MWCNT diameter can vary significantly and as a result a very broad range of FE characteristics are present in the literature. The value of E_{to} can vary from ~2 to 10 V m^{-1} depending upon the diameter, orientation, coverage, and geometry of the carbon nanotubes.[3,40,41] Therefore, the chemical attachment of SWCNT, DWCNT, and MWCNTs to Si is a simple method to produce FE electrodes with comparable properties to other CNT FE electrodes fabricated using more sophisticated methods.

The emission properties of Si-CNT surfaces can be further compared to inorganic semiconducting nanostructures, such as nanowires, nanorods, nanoscrews, and nanotubes. The range of materials is vast and the emission characteristics

TABLE I. Summary of field emission characteristics for SWCNT, DWCNT, and MWCNTs chemically attached to silicon.

CNT type	CNT diameter (nm)	D/G ratio	β	$E_{to\ 10\mu A\ cm^{-2}}$ (V μm^{-1})	$E_{to\ 100\mu A\ cm^{-2}}$ (V μm^{-1})	$E_{to\ 500\mu A\ cm^{-2}}$ (V μm^{-1})
SW	1.5	0.08	5587 ± 1571	1.29 ± 0.042	2.1 ± 0.357	2.85
DW	<5	0.27	4748 ± 1133	1.91 ± 0.165	2.51 ± 0.265	2.97
MW	>20	1.04	3069 ± 1150	2.79 ± 0.62	3.03 ± 0.147	3.54

of some structures rival that of SWCNTs with E_{to} values of ~1–20 V μm^{-1} recorded depending upon the shape and composition of the nanostructure.[42,43]

Field emission from the samples could be improved by decoration of the sidewalls with nanoparticles, which has previously been shown to improve the FE of DWCNTs.[38] The carboxylic acid groups on the sidewalls of the CNTs could be used to chemically attach nanoparticles to the sidewalls. The FE properties could also potentially be improved by the removal of the functional groups by heating the sample over 500 °C. This has previously been shown to lower the E_{to} by ~55%.[44,45]

Although the Si-MWCNT electrode exhibited the least advantageous FE characteristics, the cost of the raw MWCNT material is much less than for the SWCNTs and DWCNTs. Depending upon the device, it may be more financially viable to use MWCNTs and a higher applied electric field to produce the same electron source.

The chemically attached CNTs on the surface have a much lower height (<100 nm) than most CNT FE electrodes (generally >1 μm) this could be potentially advantageous in the implementation of these surfaces in a field emission device. With the low CNT height, a very small cathode-to-anode distance (~1 μm) can be used, which will create an electron source that requires a very low applied voltage to achieve a high electric field.

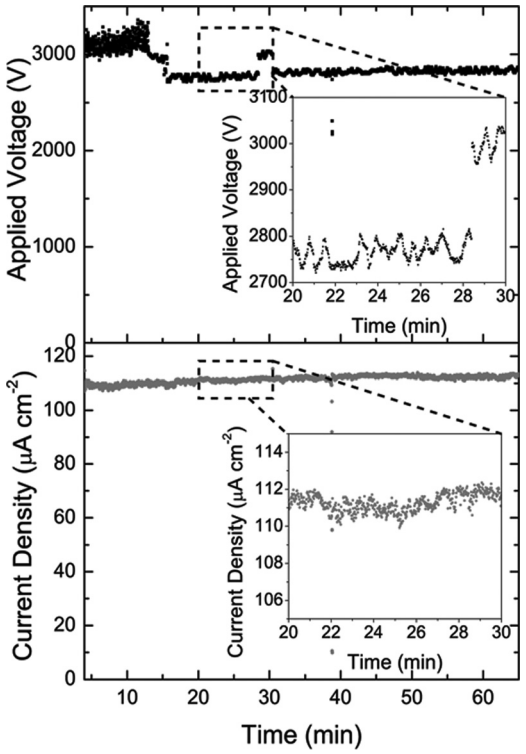

FIG. 5. Stability test of Si-SWCNT sample at constant supplied current of ~100 μA for 60 min.

C. Field emission stability

We have previously reported Si-SWCNT FE stability where it was found that a FE current density of 10 μA cm^{-2} could be maintained for over 40 h without a noticeable difference in applied voltage. A similar stability test at a higher current output was completed where the FE current was maintained at 100 μA cm^{-2} for over 60 h where it was found that an increase in applied voltage of 8.6% within the first 2 h, 15% within the first 15 h and a total of 25.8% for the entire 65 h occurred.[15]

The stability of the emission from each CNT type was investigated by setting a constant input current and monitoring the FE current output and change in voltage required to maintain that current for 1 h. The emission stability test of the Si-SWCNT surface is shown in Fig. 5. After some initial instability, the input voltage required to maintain a FE current density of 110 μA cm^{-2} drops from ~3000 to ~2720 V after 15 min. The input voltage then becomes quasi-stable with oscillations of ±40 V (1.5%), whereas the voltage slowly increases for the remainder of the test to 2860 V. The overall change in applied voltage is a decrease of 140 V (4.9%). After the initial instability the increase in voltage from 15 to 60 min is 140 V (5.1%).

The emission from the Si-SWCNT surface is remarkably stable when compared to most other SWCNT devices and is greater than previously reported.[15] The improvement of the stability from our previous work lies in the 2 h SWCNT attachment time used, which has been shown to be the attachment time that produces the best photovoltaic[14] and electrochemical devices.[21,46] The emission stability of these Si-SWCNT devices is attributed to the chemical attachment process in which the SWCNTs are bound to the substrate via a chemical bond, reducing the likelihood of SWCNT desorption during FE (a common emission degradation mechanism)[47] and subsequently improving emission stability. This is in direct contrast to CVD grown systems where the lack of adhesion between the substrate and the CNTs can be a major issue.[5]

The FE stability test of the Si-DWCNT electrode is shown in Fig. 6. During the test, the applied voltage increased from 4330 to 4450 V (2.8% increase), simultaneously maintaining a FE current density of 85 μA cm^{-2}. After an initial voltage drop to 4220 V after 5 min the voltage increased by 5.5% for the remainder of the test. The difference in FE current density between the Si-SWCNT and Si-DWCNT samples investigated comes from the sample size; the FE current from both samples was 100 μA. Throughout the stability test the voltage value oscillated by ±50 V (1%).

It was surprising to observe that the Si-DWCNT electrode had poorer emission stability than the Si-SWCNT electrode. In addition, a number of sharp voltage/current spikes, where both the current and voltage suddenly drop, can be observed in the data (e.g., at 5 and 20 min). Interestingly, only a single such event was observed for the entire duration of the stability test conducted on the Si-SWCNT surface.

Previous work on FE from CNT arrays has shown that these spikes are due to CNT fragments that are ejected from the surface.[48] Given that the chemical attachment should restrict entire CNTs from desorbing, the most likely scenario is that fragments of the CNTs are being "pulled" from the surface. The DWCNTs have a higher degree of functionalization than the SWCNT (as determined by the D/G ratio from the Raman data) and increased functionalization has

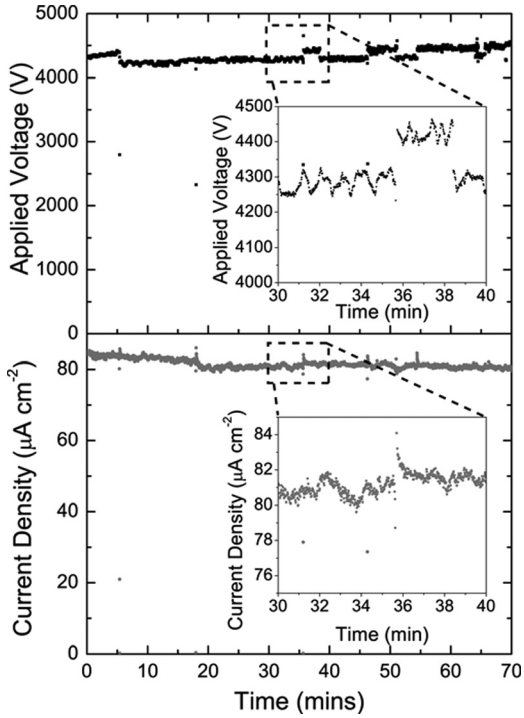

FIG. 6. Stability test for Si-DWCNT sample at a constant supplied current of 100 μA for 70 min.

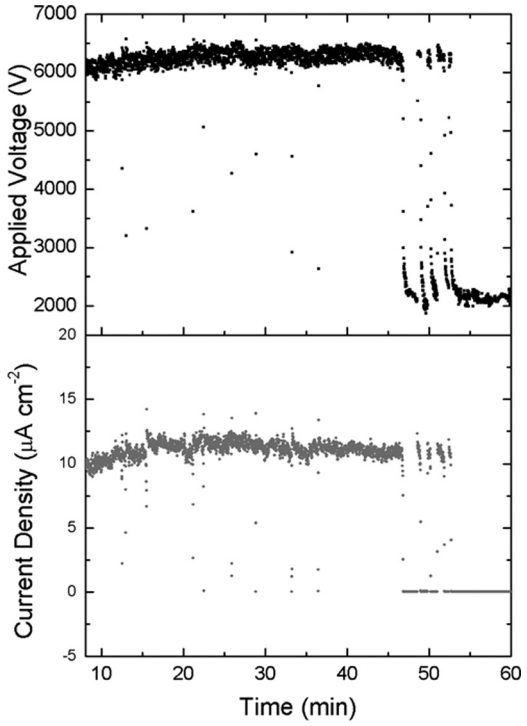

FIG. 7. Stability test for Si-MWCNT sample at a constant current of 10 μA for ~50 min.

been shown previously to reduce the emission stability from CNT surfaces.[49,50] It has been reported that these defect sites led to increased joule heating, which in turn leads to field evaporation from the CNT, which subsequently lowers emission stability.[47] Although the DWCNTs have an extra shell to reduce the effects of ion bombardment, the increased functionality (which was required to chemically attach them to the surface) and subsequent reduction in CNT crystallinity leads to the Si-DWCNT electrodes having poorer FE stability than the Si-SWCNT surfaces.

The stability test of the Si-DWCNT electrode was continued for over 15 h (data not shown) where the applied voltage rose from 4200 to 4650 V (10% increase) and the FE current density dropped from 85 to 70 μA cm^{-2} (18% decrease). The supplied current was constant but the FE current decreased due to a gradual change in resistance of the sample as the number of emitters decreased.

A 100 μA cm^{-2} FE stability test for the Si-MWCNT electrode could not be achieved as the sharp voltage/current spike events (such as those observed for the Si-DWCNT electrode) occurred on a regular basis (~1 per 5 s) and eventually the LabView program would fail to restore the current. Instead, a 1 h 10 μA cm^{-2} FE stability test for the Si-MWCNT surface is shown in Fig. 7. The applied voltage is quasi-constant for the first 45 min of the test with a constant oscillation of $\pm$175 V (3%), after which time the emission cycles through four failures and recoveries prior to a final failure from which the LabView program could not resurrect emission. Throughout the first 45 min of the stability test, 11 sharp current/voltage drop events are observed. These drops are similar to that observed for the Si-DWCNT electrode, but are more than twice as frequent. Considering the lower applied load to the surface (10% of current density), the volume of material being ejected from the surface is comparatively high. This observation is consistent with the mechanism proposed for the degradation of emission for the Si-DWCNT or Si-SWCNT electrodes and, as such, the defect/functionalization population on the MWCNT is much greater. The greater number of defect sites (lower crystallinity) will increase the effect of joule heating and lead to a higher amount of CNT field evaporation and the lower emission stability of the device. The event at 45 min (Fig. 7), where the output current dropped to zero, is not an irreversible failure of the system because subsequent *I–V* sweeps showed FE characteristics similar to before the stability test. Repeated experiments observed similar failure events.

The FE emission stability characteristics observed are contradictory to previously reported findings where it is expected that FE from MWCNT emitters is more stable than from SWCNT emitters.[3] FE stability is affected by a number of variables including CNT adhesion, ohmic contact, ion bombardment, and CNT crystallinity. Within this study, CNT adhesion and ohmic contact is constant between CNT types as SWCNT, DWCNT, and MWCNT substrates were prepared via identical chemical attachment. The effect of ion bombardment is reported to be reduced by the extra shells of MWCNTs,[47] thus the lower emission stability observed for the Si-MWCNT substrate cannot result from ion bombardment. The crystallinity of the CNTs is affected by both their original manufacturing process and functionalization. The DWCNT and MWCNTs were originally produced by CVD, which is a process known to produce CNTs with lower crystallinity than arc-discharge, which was used to produce the SWCNTs. The size of the D-band after CNT functionalization in the Raman data further confirms that the crystallinity of the DWCNTs and MWCNTs is lower than for the

SWCNT sample (Table I). Therefore, the observed trend of emission stability relating to the original CNT crystallinity is expected. Future work in this field could involve the chemical attachment and investigation of field emission properties of highly crystalline MWCNTs and DWCNTs produced by arc-discharge.

IV. CONCLUSIONS

Chemically functionalized SWCNTs, DWCNTs, and MWCNTs were chemically attached to silicon. Attachment and alignment were monitored by AFM, where it was found that alignment varied between the CNT types. CNT type and diameter were probed by Raman spectroscopy, where it was confirmed that SWCNTs, DWCNTS, and MWCNTs surfaces were produced. Field emission experiments were completed for all CNT types where the values of E_{to} from 1.28 V μm^{-1} (SWCNT) to 1.91 V μm^{-1} (DWCNT) and 2.79 V μm^{-1} (MWCNT) were recorded, whereas β was found to change from 5587 to 4748 to 3069 for the SWCNT, DWCNT, and MWCNT surfaces, respectively. Changes in the FE characteristics directly correlated to changes in CNT diameter and alignment as shown by Raman and AFM. The FE from SWCNTs was shown to be more stable than from DWCNTs, which was far more stable than from MWCNTs. The emission stability characteristics observed are contradictory to previously reported findings, where it is expected that MWCNT are superior to SWCNTs. The chemical functionalization has been shown to play a role in the emission stability with higher functionalization, and hence lower CNT crystallinity, leading to poorer emission stability. The chemical attachment of CNTs to Si is an upscaleable approach to producing efficient field emission surfaces.

[1]A. G. Rinzler, J. H. Hafner, P. Nikolaev, P. Nordlander, D. T. Colbert, R. E. Smalley, L. Lou, S. G. Kim, and D. Tomanek, Science **269**, 1550 (1995).
[2]B. Q. Wei, R. Vajtai, and P. M. Ajayan, App. Phys. Lett. **79**, 1172 (2001).
[3]J. M. Bonard, H. Kind, T. Stokli, and L.-O. Nilsson, Solid State Electron. **45**, 893 (2001).
[4]R. C. Smith, J. Appl. Phys. **106**, 014314 (2009).
[5]A. Pandey, A. Prasad, J. P. Moscatello, and Y. K. Yap, ACS Nano **4**, 6760 (2010).
[6]J. M. Bonard, M. Croci, C. Klinke, R. Kurt, O. Noury, and N. Weiss, Carbon **40**, 1715 (2002).
[7]Y.-W. Son, S. Oh, J. Ihm, and S. Han, Nanotechnology **16**, 125 (2005).
[8]S. Fan, M. G. Chapline, N. R. Franklin, T. W. Tombler, A. M. Cassell, and H. Dai, Science **283**, 512 (1999).
[9]C. Xiomara, X. Calderón-Colón, H. Geng, B. Gao, L. An, G. Cao, and O. Zhou, Nanotechnology **20**, 325707 (2009).
[10]K. T. Constantopoulos, C. J. Shearer, A. V. Ellis, N. H. Voelcker, and J. G. Shapter, Adv. Mater. **22**, 557 (2010).
[11]L. B. Zhu, Y. Y. Sun, D. W. Hess, and C. P. Wong, Nano Lett. **6**, 243 (2006).
[12]J. Yu, J. G. Shapter, J. S. Quinton, M. R. Johnston, and D. A. Beattie, Phys. Chem. Chem. Phys. **9**, 510 (2007).
[13]J. Yu, J. G. Shapter, M. R. Johnston, J. S. Quinton, and J. Gooding, Electrochim. Acta **52**, 6206 (2007).
[14]M. A. Bissett and J. G. Shapter, J. Phys. Chem. C **114**, 6778 (2010).
[15]C. J. Shearer, J. G. Shapter, J. S. Quinton, P. C. Dastoor, L. Thomsen, and K. M. O'Donnell, J. Mater. Chem. **18**, 5753 (2008).
[16]M. Marshall, S. Popa-Nita,and J. G. Shapter, Carbon **44**, 1137 (2006).
[17]D. K. Aswal, S. Lenfant, D. Guerin, J. V. Yakhmi, and D. Vuillaume, Anal. Chim. Acta **568**, 84 (2006).
[18]P. Diao and Z. Liu, Adv. Mater. **22**, 1430 (2010).
[19]Z. Liu, Z. Shen, T. Zhu, S. Hou, and L. Ying, Langmuir **16**, 3569 (2000).
[20]B. Wu, J. Zhang, Z. Wei, S. Cai, and Z. Liu, J. Phys. Chem. B **105**, 5075 (2001).
[21]B. S. Flavel, J. Yu, J. G. Shapter, and J. S. Quinton, Carbon **45**, 2551 (2007).
[22]J. Yu, S. Mathew, B. S. Flavel, M. R. Johnston, and J. G. Shapter, J. Am. Chem. Soc. **130**, 8788 (2008).
[23]C. J. Shearer, A. V. Ellis, J. G. Shapter, and N. H. Voelcker, Langmuir **26**, 18468 (2010).
[24]H. L. Young, H. A. Kay, S. P. Jin, Y. Cheol-Min, Y. J. Seung, C. L. Seong, K. Chul, S. Joo-Hiuk,and J. Mun Seok, J. Am. Chem. Soc. **127**, 5196 (2005).
[25]H. L. Young, S. Kwanyong, A. P. Kyung, K. Changwook, H. Seungwu, and K. Bongsoo, J. Am. Chem. Soc. **127**, 15724 (2005).
[26]M. S. Dresselhaus, G. Dresselhaus, R. Saito, and A. Jorio, Phys. Rep. **409**, 47 (2005).
[27]D. A. Heller, P. W. Barone, J. P. Swanson, R. M. Mayrhofer, and M. S. Strano, J. Phys. Chem. B **108**, 6905 (2004).
[28]S. Chakrabarti, K. Gong, and L. Dai, J. Phys. Chem. C **112**, 8136 (2008).
[29]See supplementary material at http://dx.doi.org/10.1063/1.3687363 for Raman spectra and analysis of raw DWCNTs showing the extra RBM peaks that are hidden by the silicon peaks in the Si-DWCNT electrodes.
[30]J.-P. Salvetat, A. J. Kulik, J.-M. Bonard, G. A. D. Briggs, T. Stöckli, K. Méténier, S. Bonnamy, F. Béguin, N. A. Burnham, and L. Forró, Adv. Mater. **11**, 161 (1999).
[31]N. Jonge, M. Allioux, M. Doytdcheva, M. Kaiser, K. B. K. Teo, R. G. Lacerda, and W. I. Milne, App. Phys. Lett. **85**, 1607 (2004).
[32]X. Lu, Q. Yang, C. Xiao, and A. Hirose, J. Phys. D **39**, 3375 (2006).
[33]W. Liang, M. Bockrath, D. Bozovic, J. H. Hafner, M. Tinkham, and H. Park, Nature (London) **411**, 665 (2001).
[34]P. Liu, Q. Sun, F. Zhu, K. Liu, K. Jiang, L. Liu, Q. Li, and S. Fan, Nano Lett. **8**, 647 (2008).
[35]S. C. Youn, D.-H. Jung, Y. K. Ko, Y. W. Jin, J. M. Kim, and H.-T. Jung, J. Am. Chem. Soc. **131**, 742 (2008).
[36]Y. Chen, H. Miao, R. J. Lin, M. Zhang, R. Liang, C. Zhang, and B. Wang, Nanotechnology **21**, 495702 (2010).
[37]Y. Chen, H. Miao, R. J. Lin, M. Zhang, R. Liang, C. Zhang, and B. Wang, Nanotechnology **19**, 415703 (2008).
[38]C. Liu, K. S. Kim, J. Baek, Y. Cho, S. Han, S.-W. Kim, N.-K. Min, Y. Choi, J.-U. Kim, and C. J. Lee, Carbon **47**, 1158 (2009).
[39]B. Ha, D. H. Shin, J. Park, and C. J. Lee, J. Phys. Chem. C **112**, 430 (2007).
[40]G. Chen, D. H. Shin, S. Kim, S. Roth, and C. J. Lee, Nanotechnology **21**, 015704 (2010).
[41]R. Seelaboyina, S. Boddepalli, K. Noh, M. Jeon, and W. Choi, Nanotechnology **19**, 065605 (2008).
[42]X. Fang, Y. Bando, U. K. Gautam, C. Ye, and D. Golberg, J. Mater. Chem **18**, 509 (2008).
[43]B. Cao, X. Teng, S. H. Heo, Y. Li, S. O. Cho, G. Li, and W. Cai, J. Phys. Chem. C **111**, 2470 (2007).
[44]H. Wang, Z. Li, K. Ghosh, T. Maruyama, S. Inoue, and Y. Ando, Carbon **48**, 2882 (2010).
[45]S. I. Jung, S. H. Jo, H. S. Moon, J. M. Kim, D.-S. Zang, and C. J. Lee, J. Phys. Chem. C **111**, 4175 (2007).
[46]B. S. Flavel, J. Yu, J. G. Shapter, and J. S. Quinton, Electrochim. Acta **53**, 5653 (2008).
[47]J. M. Bonard, C. Klinke, K. A. Dean, and B. F. Coll, Phys. Rev. B **67**, 115406 (2003).
[48]K. M. O'Donnell, Ph.D.thesis, University of Newcastle, Callaghan, NSW, Australia, 2010.
[49]C. Y. Zhi, X. D. Bai, and E. G. Wang, Appl. Phys. Lett. **81**, 1690 (2002).
[50]B. Ulmen, V. K. Kayastha, A. DeConinck, J. Wang, and Y. K. Yap, Diamond Relat. Mater. **15**, 212 (2006).